# Positional reorganization in compound *janus* cells of *Tetrahymena thermophila*

JOSEPH FRANKEL and E. MARLO NELSEN

*Department of Biology, University of Iowa, Iowa City, Iowa 52242, USA*

## Summary

The *janus* mutations of *Tetrahymena thermophila* convert the large-scale organization of the dorsal surface of the cell into a mirror-image of the ventral surface, which is characterized by a second, abnormal, oral apparatus and by contractile vacuole pores to the left of the second oral area rather than the usual right. This conversion could be due either to a local change in the response to an unaltered positional system or to a more global reorganization of the system itself. *janus* homopolar doublets were used to distinguish between these two alternatives. Homopolar doublets can be made by fusing two similarly oriented cells in side-by-side parabiosis. Non-*janus* homopolar doublets typically possess two sets of normal oral structures with contractile vacuole pores to the right of each of them. In *janus* doublets, there are up to four sets of oral structures, with the abnormal oral structures located between the two sets of normal oral structures; contractile vacuole pores are situated to the right of the normal oral areas and to the left of the abnormal oral structures.

Non-*janus* homopolar doublets are known to propagate their compound condition for a number of cell divisions, but also to regulate toward the singlet state through a progressive reduction in number of ciliary rows followed by loss of one of the two sets of major cell surface structures. *janus* homopolar doublets go through a corresponding regulation. As a consequence, the location of the abnormal oral structures relative to the normal ones is more variable in *janus* doublets than in *janus* singlets. Sometimes the abnormal oral structures shift to a position close to their normal counterparts and then the intervening CVP sets disappear. There is evidence for occasional fusion of an abnormal oral area with an adjacent normal oral apparatus, a condition that may be transitional to the singlet state. These observations are inconsistent with the idea of a fixed positional system and strongly suggest a global reorganization of the surface pattern in a manner consistent with predictions of an intercalation model that was first proposed to explain the regulation of non-*janus* doublets to singlets.

Key words: pattern formation, ciliate, *Tetrahymena thermophila*, patterning, cell surface, spatial organization.

## Introduction

Disruptions of spatial patterns in organisms expressing mutations can be due either to alterations of a large-scale positional system or to defects in local cellular responses to an unaltered positional system (Stern, 1954). For zygotically acting mutations of *Drosophila* and other multicellular organisms, the two alternatives can be distinguished operationally by examining phenotypes of genetic mosaics: effects on large-scale 'prepattern' (Stern, 1954) or 'positional information' (Wolpert, 1971) should result in abnormality in both wild-type and mutant tissue (nonautonomy), whereas local effects on cellular 'response'

(Stern, 1954) or 'interpretation' (Wolpert, 1971) should bring about abnormality restricted to mutant tissue (autonomy). The typical outcome of tests of these alternatives has been autonomous expression (Stern, 1968; Tokunaga, 1978), even for mutations affecting an event as early as embryonic segmentation (Gergen & Wieschaus, 1985, 1986).

A major limitation of analysis of genetic mosaics is that it requires gene expression after multicellularity has been achieved. Even in multicellular organisms such as *Drosophila*, the mutations most likely to affect large-scale positional systems are those that alter the organization of the egg. As these mutations act prior to fertilization, their effects within the egg cannot be

analysed in genetic mosaics. These defects have been analysed by other means, with results suggesting large-scale effects on positional systems (Anderson & Nüsslein-Volhard, 1986; Mohler & Wieschaus, 1986).

In the ciliate *Tetrahymena thermophila*, the *janus* mutations (Frankel & Jenkins, 1979, and unpublished data) convert the global organization of the dorsal (aboral) surface of the cell into a mirror image of that of the ventral (oral) surface (Jerka-Dziadosz & Frankel, 1979; Frankel, Jenkins & Bakowska, 1984). The *janus* phenotype can be interpreted in two general ways. The first is to postulate the existence of two preformed boundary zones, one along the mid-ventral (oral) meridian of the cell and the other along the mid-dorsal (aboral) meridian which, like the anterior and posterior ends of the insect egg (Sander, 1960), could be envisaged as organizing centres for oppositely directed gradients. Relevant genes could then influence an 'oral–aboral decision' at these predetermined meridians. This idea, analogous to that of an 'anterior–posterior decision' postulated by Kalthoff (1979) for the poles of the insect egg, would give the wild-type products of the *janus* genes roles in the suppression of a latent capacity of a mid-dorsal region to switch to a midventral state of expression; the mutant phenotype would result from failure to exert this suppression. In this view, the *janus* genes would influence only the interpretation of stable positional information.

A second possibility is that there are no stable boundaries, but instead the oral meridians are expressions of a global positional system obeying certain rules of spacing and continuity. The wild-type products of the *janus* genes would be required to maintain the normal organization of this system. Mutations at these loci would affect portions of the positional system and thereby trigger a reorganization of the whole system. In this view, the products of the *janus* genes are intimately involved in maintaining the organization of an intracellular positional system.

Although we originally favoured the first alternative (Frankel & Nelsen, 1981), a more thorough analysis of how one *janus* mutation (*janA1*) comes to expression supported the second view (Frankel & Nelsen, 1986*b*). The evidence, however, was not completely decisive.

The ability of ciliates, including *Tetrahymena*, to propagate variant structural configurations offers a unique opportunity for distinguishing between these two alternatives. The elaborate structural organization of the ciliate cell surface is normally perpetuated during growth and division. A classic example of such perpetuation is the propagation of the difference
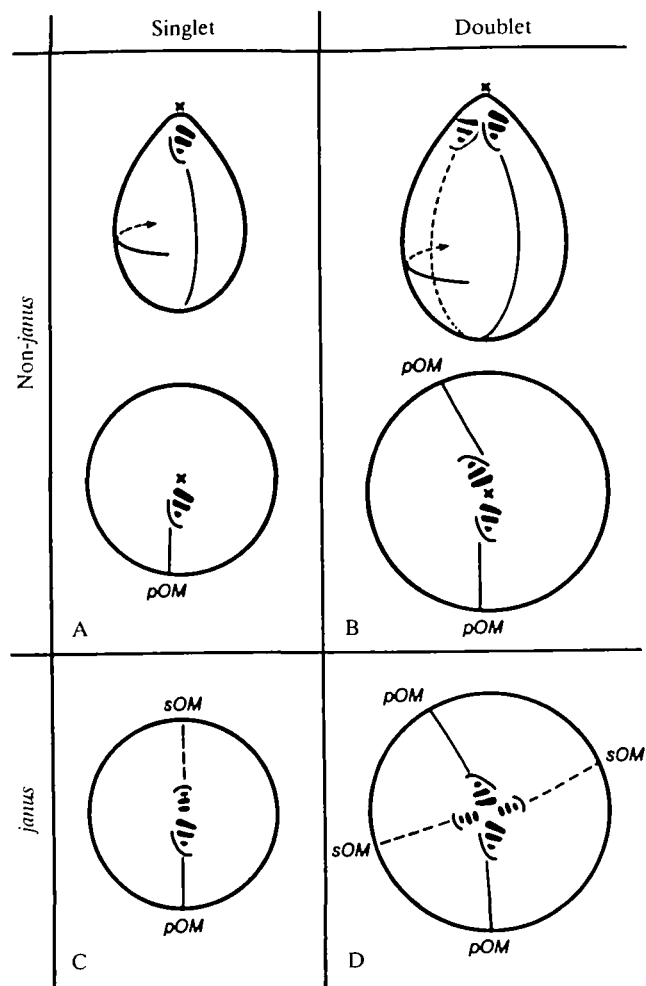


Fig. 1. Diagrammatic summaries of the geometrical arrangements of oral structures and oral meridians in non-*janus* singlets (A), non-*janus* homopolar doublets (B), *janus* singlets (C), and *janus* homopolar doublets (D). In panels A and B, the same cells are illustrated in schematic lateral views assuming transparency (above) and in polar projections (below). The anterior end of the cell is marked with an 'x' in both representations in panels A and B. In the polar projections, the solid radii indicate primary oral meridians (*pOM*) characterized by normal oral structures, while the dashed radii indicate secondary oral meridians (*sOM*), characterized by abnormal, partially reversed, oral structures. For further explanation, see the text.

between singlet and homopolar-doublet cells, respectively characterized by one (Fig. 1A) and two (Fig. 1B) oral meridians (Sonneborn, 1963). However, transformation of pattern can and does occur. Homopolar doublets, which can be constructed by lateral fusions of singlets, tend to regulate back to the singlet state over the course of several successive rounds of cell division. This phenomenon has been documented extensively in *Tetrahymena* (Fauré-Fremiet, 1948; Nanney, 1966*a*; Nanney, Chow

& Wozencraft, 1975; Nelsen & Frankel, 1986). Such regulation must involve the eventual loss or suppression of one oral meridian.

Cells expressing a *janus* allele (Fig. 1C) can best be thought of as singlets with a reversed ('secondary') oral meridian on the previous dorsal surface (Frankel & Nelsen, 1986*b*). They differ fundamentally from non-*janus* homopolar doublets (Fig. 1B) not only in their geometry but also in their stability. The *janus* condition is genotypically controlled and persists indefinitely whereas the homopolar doublet state is maintained by structural inertia and is unstable. The two conditions are not mutually exclusive; that is, one can, by lateral fusion, generate 'double-*janus*' cells (Fig. 1D) which stand in the same geometrical relation to 'single-*janus*' cells (Fig. 1C) as non-*janus* homopolar doublets (Fig. 1B) do to non-*janus* singlets (Fig. 1A). Just as non-*janus* homopolar doublets are known to regulate to normal singlets, *janus* homopolar doublets would be expected to regulate to *janus* 'singlets', losing one normal ('primary') and one reversed ('secondary') oral meridian.

An analysis of the process by which loss of both types of oral meridians occurs permits us to make a judgement of whether pattern boundaries are fixed or labile. We will show that the pattern boundaries are labile and that the manner by which *janus* doublets regulate to *janus* singlets is predictable from a model in which the original *janus* organization is due to a global reordering of positional values caused by failure to maintain a subset of these values.

## Materials and methods

### Stocks

The two stocks used in this investigation were both *Tetrahymena thermophila* of the inbred B strain. One of them, IA203, is homozygous for *janA1* (the former *janus*) and for an 'enhancer of *janA*' (*eja*) (Frankel, Jenkins & Bakowska, 1984). The other, IA207, is triply homozygous for *janA1*, *eja*, and the fission-arrest mutation *cdaA2* [formerly *mol*[b] (Frankel, Jenkins, Doerder & Nelsen, 1976)].

### Media and experimental procedures

Stock cultures were maintained in culture tubes containing '1 % PPY' medium, consisting of 5 ml of 1 % proteose peptone (Difco) plus 0·1 % bactoyeast extract (Difco). Phenotypes were assessed in an enriched 'PPYGFe' medium containing 2 % proteose peptone, 0·2 % yeast extract, 0·5 % glucose and an iron-chelate complex (Nelsen, Frankel & Martel, 1981).

Homopolar doublets were obtained by a slight modification of one of the methods of Nelsen & Frankel (1986). Very early exponential phase cultures initially grown in 1 % PPY at 30°C were then maintained at 39°C for about 7 h to bring about blockage of fission in most cells. Following this

heat treatment, cultures were returned to room temperature (about 22°C). Drops of this culture were transferred aseptically to wells in three-spot depression slides ('spot plates', Corning no. 7223) and fresh 1 % PPY was added to the wells. Growth in 1 % PPY results in low expression of the aberrant shape associated with the *janA1* phenotype, assuring easy selection of homopolar doublets. The depression slide cultures were maintained without antibiotics in a moist chamber within an air-curtain incubator ('Edgegard', Baker Co., Sanford, ME) at room temperature (about 22°C). After one day of growth, homopolar doublets were selected on the basis of a *Stentor*-like appearance (Nelsen & Frankel, 1986). Not more than one homopolar doublet was selected from each well. The doublets were transferred individually to fresh wells of 1 % PPY and maintained at room temperature. Approximately 3 days later, clones that appeared to have many homopolar doublets were transferred *en masse* to 5 ml tubes of PPYGFe and placed at a slant in a 30°C incubator to promote rapid culture growth and high expression of the *janA* phenotype. These cultures were fixed the next day, while in exponential phase of culture growth (roughly 18 generations after cloning and 22 generations after the heat treatment), and prepared for light microscopical examination using the Chatton–Lwoff silver impregnation method following the procedure of Frankel & Heckmann (1968), as modified by Nelsen & DeBault (1978).

The extent to which the usual expression of *janA1* is modified by combination with *cdaA2* was assessed in a separate experiment, in which cells of stocks IA203 (*janA1/janA1 cdaA*[+]/*cdaA*[+]) and IA207 (*janA1/janA1 cdaA2/cdaA2*) were grown overnight in 150 ml samples of PPYGFe medium in 450 ml Fernbach flasks, and fixed for silver impregnation the following morning, while in exponential phase of culture growth.

### Nomenclature and procedures for assessment of cytogeometry

The major structural elements of the cell surface of *Tetrahymena thermophila* are the ciliary rows, oral apparatus (OA), oral primordium (OP), and contractile vacuole pores (CVPs) (Fig. 2). A singlet cell typically possesses 18 to 21 longitudinal ciliary rows; the term 'corticotype' (Nanney, 1966*a*) will be used as a shorthand expression for the number of these rows. The OA is a compound ciliary structure located near the anterior end of the cell, normally with three ciliary assemblages known as membranelles (M1, M2, M3) on its left side and another kind of ciliary assemblage known as an undulating membrane (UM) on its right (throughout this paper, 'right' and 'left' are defined as viewed from the cell interior looking outwards). While most ciliary rows extend from the anterior to the posterior end of the cell, two postoral ciliary rows begin from the posterior margin of the OA. The right postoral (RP) row is numbered 1; numbering proceeds around to the cell's right, so that the left postoral (LP) row is numbered n. In typical cells, CVPs are located close to the posterior ends of one, two, or three adjacent ciliary rows (CVP rows).

Before fission begins, new basal bodies are added within ciliary rows. A new oral primordium (OP) develops, typically to the cell's left of the midregion of the right
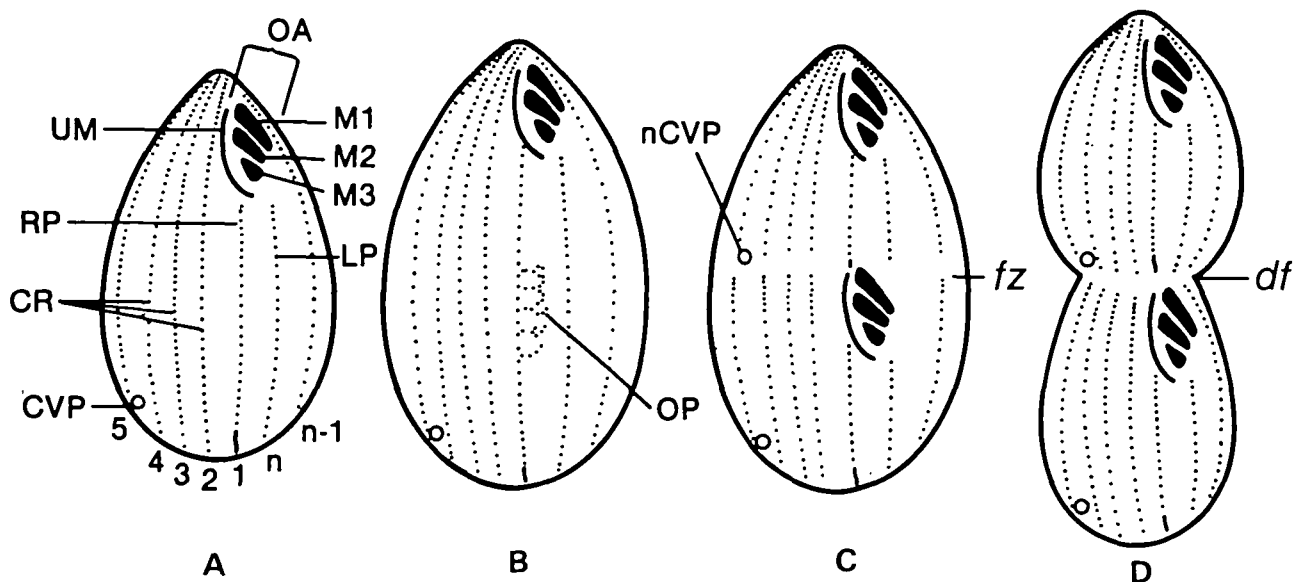
Fig. 2. Diagrams of structural features of the ventral surface of *Tetrahymena thermophila* at different stages of cell surface development. Seven longitudinal ciliary rows (CR) are shown, including the right postoral (RP) and left postoral (LP) rows. The RP row is the reference point for the numbering scheme shown beneath the rows in diagram A. The oral apparatus (OA) is made up of four sets of closely spaced basal bodies, three membranelles (M1, M2, M3) and the undulating membrane (UM). One of the contractile vacuole pores (CVP) is visible. (A) The cell surface prior to the onset of predivision oral development. (B) Early oral development (stage 1), with an oral primordium (OP) appearing at midbody adjacent to the RP ciliary row. (C) The late predivision stage of oral development (stage 5). An equatorial fission zone (fz) appears anterior to the nearly fully differentiated oral primordium. New CVPs (nCVP) are formed just anterior to the fission zone. (D) The division stage (stage 6), with a constricting division furrow (df). Redrawn from Frankel & Nelsen, 1986*b*.

postoral ciliary row (Fig. 2B). The OP forms initially as a field of basal bodies, which then become organized into the membranelles and UM of the future posterior division product [Fig. 2C; for details see Lansing, Frankel & Jenkins (1985)]. When the organization of the OP is nearly complete, an equatorial fission zone appears, which splits the ciliary rows into anterior and posterior portions. At this time new CVPs develop anterior to the discontinuity in the ciliary rows, next to the most posterior basal bodies of the CVP rows (Ng, 1979). The cell then is cleaved along the fission zone (Fig. 2D).

The *Tetrahymena* cell thus grows longitudinally and divides transversely. During this growth and division, the ciliary rows retain their continuity as new ciliary units are added, whereas OAs and CVP sets are formed anew near the prospective fission zone, far from old structures of the same kind. The structures in each daughter cell are thus of different ages: the anterior division product has an old OA and new CVPs, while the posterior division product has a new OA and old CVPs.

Occasionally an OP develops along a ciliary row other than the right postoral row. This is termed 'cortical slippage' (Nanney, 1967). New CVPs may also develop along ciliary rows different from old ones.

Polar projections are used to illustrate schematically the distribution of structures around the cell circumference. The four basic configurations shown in Fig. 1 are repeated in Fig. 3, with CVPs and terminology added. The basic subdivisions of the cell circumference are defined by

locations of the oral meridians. A primary oral meridian (*pOM*) is defined by the right postoral ciliary row (no. 1) of a normal, primary OA (pOA) or OP (pOP, not shown), while a secondary oral meridian (*sOM*) is defined by the single postoral ciliary row of an abnormal, secondary OA (sOA) or OP (sOP, not shown). The space (measured in ciliary row intervals) between two primary oral meridians is defined as a semicell (*sc*). When the two primary oral meridians are not directly opposite one another, the doublet is called unbalanced (see Nelsen & Frankel, 1986) and the narrower semicell is arbitrarily designated as semicell 1 (*sc1*), the wider semicell as semicell 2 (*sc2*) (Fig. 3B,D). The primary oral meridian with *sc1* to its right is labelled 1 (*pOM1*), while the primary oral meridian with *sc2* to its right is labelled 2 *(pOM2)*. A secondary oral meridian within *sc1* is called *sOM1* and a secondary oral meridian within *sc2* is called *sOM2* (Fig. 3D). The space between a primary and a secondary oral meridian is called a sector. A *janus* singlet (Fig. 3C) is divided into two sectors, *sr1* to the right of the *pOM* and the left of the *sOM*, and *sr2* to the left of the *pOM* and the right of the *sOM*. In *janus* doublets (Fig. 3D), sectors are nested within the semicells. To distinguish the sectors within the two semicells, *sr1* within *sc1* is named *sr11*, *sr1* within *sc2* is named *sr12*, *sr2* within *sc1* is named *sr21*, and *sr2* within *sc2* is named *sr22*.

Ciliary rows bearing CVPs are called CVP rows. The CVP arc is defined as the set of ciliary rows that is bounded by the outermost CVP rows of a group. In *janus* cells, the CVP arc may include 'skipped' rows that lack CVPs, as

shown in Fig. 3C,D. The CVP midpoint (*CM*) is the mean location of all of the CVP rows within the CVP arc, including skipped rows if any are present. *d* represents the distance, in ciliary row intervals, between the *pOM* and the *CM*. In doublets, where more than one CVP set is present, these sets are identified according to the semicells (*not*

sectors) in which they are located; thus CVP arc 2, *CM2* and *d2* refer to features of CVPs in *sc2* (Fig. 3B,D).

These measurements allow the computation of relative positions of structures. By convention, these relative positions are always computed using ciliary-row counts made to the right of the relevant reference point. The ones to be
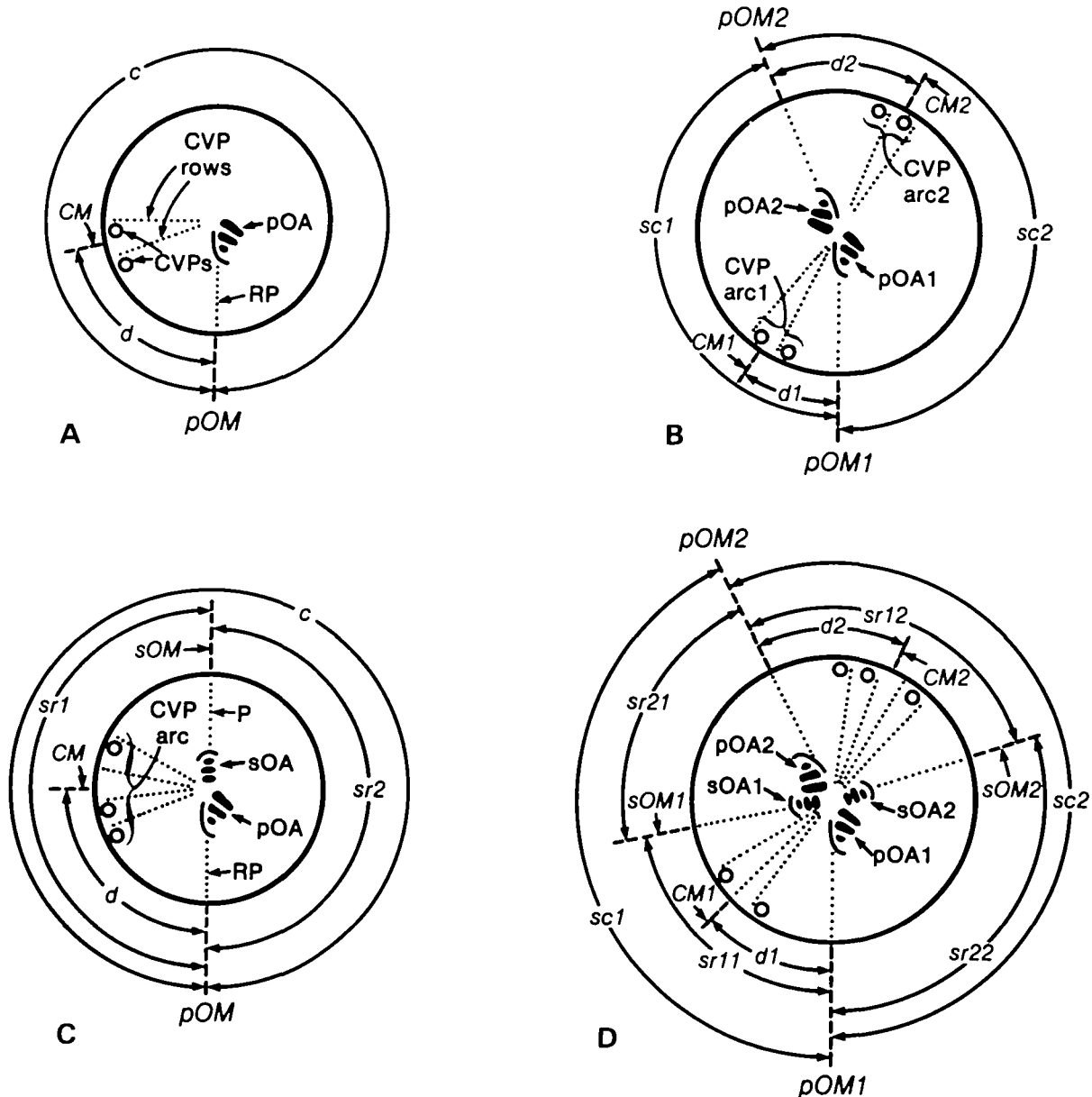


**Fig. 3.** Labelled polar projections of the four structural configurations shown in Fig. 1. Cell structures are labelled by standard letters inside the diagrams, while reference locations are labelled by italicized capital letters and distances between these locations by lower-case italics, both outside the diagrams. The diagrams show primary oral areas (pOA), secondary oral areas (sOA), contractile vacuole pores (CVP), and selected ciliary rows: the right postoral (RP) row posterior to each pOA, the single postoral row (P) posterior to each sOA, and the ciliary rows adjacent to CVPs (CVP-rows). The CVP arcs (see text for definition) are labelled in panels B and C. The three types of reference locations are the *pOM*, designating a primary oral meridian; the *sOM*, designating a secondary oral meridian; and the *CM*, designating the geometrical midpoint of a CVP arc. The four types of distances are *c*, the circumference of a cell that has only one *pOM*; *sc* (semicell), the distance between two *pOM*s; *sr* (sector), the distance between a *pOM* and an *sOM*; and *d*, the distance between a *pOM* and the *CM* of the CVP-set on its right. The rules for assigning numbers to reference locations and distances in compound cells are described in the text.

used are, first, the relative position of an sOM either within the whole cell of *janus* singlets (srl/c, Fig. 3C) or within a semicell of *janus* doublets (srl1/scl or srl2/sc2, Fig. 3D); second, the relative position of a CVP-midpoint either within the whole cell (d/c, Fig. 3A,C) or semicell (dl/scl or d2/sc2, Fig. 3B,D); and third, the position of a CVP-midpoint within its sector (d/srl in Fig. 3C, dl/srl1 or d2/srl2 in Fig. 3D).

## Statistical procedures

Statistical procedures were carried out as described by Sokal & Rohlf (1981). Computations were performed on an IBM-PC microcomputer employing SYSTAT (SYSTAT Inc., Evanston, IL).

## Results and discussion

(A) *The* janus *phenotype in homopolar doublets*

(1) *General configurations and corticotypes*

Eleven clones derived from doublets generated from fission-arrested cells of clone IA207 (*janA1/janA1 eja/eja cdaA2/cdaA2*) were examined. These clones all contained both doublets and singlets expressing the *janus* phenotype, in varying proportions. The doublets had a higher corticotype (total number of ciliary rows) than did singlets (Fig. 4, open bars) and showed varying degrees of imbalance in the locations of their two sets of primary oral structures. A few were balanced, with the two pOMs directly opposite each other, many were moderately unbalanced (Figs 5–7), while some were severely unbalanced, with the narrower semicell approximately one-half as wide as the wider semicell (Fig. 8). This range is the expected outcome of an initial selection of balanced doublets (Nelsen & Frankel, 1986) followed by a combination of random slippage in sites of formation of new oral structures and loss of ciliary rows (see appendix of Frankel & Nelsen, 1986a). The singlets in these clones had quite variable corticotypes (Fig. 4C), spanning the range from the corticotypes of doublets (Fig. 4A,B) to the corticotypes of the usual *janus* singlets (Fig. 4D,E), reinforcing the conclusion that they were progeny of doublet cells that were completing their regulation toward the normal singlet condition. Some *janus* singlets had corticotypes in the 30s, unusually high for singlets. Such singlets probably resulted from a combination of high corticotype and severe imbalance in antecedent doublets, a phenomenon that has occasionally been observed in non-*janus* doublet clones as well (Frankel & Nelsen, 1986a; Nelsen, unpublished data).

(2) *Expression of secondary oral structures*

Among the singlets in these clones, some possessed an sOA while others did not. This is typical of *janus* cells, in which expression of secondary oral structures is variable (Jerka-Dziadosz & Frankel, 1979; Frankel & Jenkins, 1979). Comparable variability was observed in homopolar doublets, in which secondary oral structures were sometimes present in *both* semicells (Figs 5, 7), sometimes in one semicell, either the narrower one (Figs 6, 8) or the wider one (not shown), and sometimes in *neither* semicell (not shown).

One of the eleven clones (no. 7), in which all of the configurations mentioned above were reasonably well represented, was chosen for detailed assessment. In a preliminary tally of 500 randomly chosen cells of this clone, 231 were singlets and 269 doublets. Among the singlets, 138 (60 %) possessed sOAs; this is typical of *janA1* stocks carrying *eja* grown in PPYGFe medium (Frankel, Jenkins & Bakowska, 1984). Among the 538 semicells in the 269 doublets, 128 (24 %) possessed sOAs, indicating that expression of secondary oral structures is reduced in homopolar doublets. In the 269 doublets, 14 had sOAs in both semicells, 100 had sOAs in one semicell and 155 had sOAs in neither semicell, close to the numbers expected (15·2 in both, 97·5 in one, 156·2 in neither) if expression of sOAs is independent in the two semicells of a given doublet.

In more detailed tallies of cells selected solely on the basis of the scorability of all cell surface features, we found that secondary oral structures were equally frequent in the narrower and wider semicells, even in highly unbalanced doublets. The independence of expression of secondary oral structures in the two semicells justifies consideration of semicells with sOMs (i.e. those possessing sOAs and/or sOPs) in scl and those with sOMs in sc2 as two independent data sets. In clone no. 7, widths of sc2 were similar to cell widths of typical *janus* singlets (Fig. 4: compare shaded bars in panel B with the open bars in panels D and E) while scl was generally considerably narrower (Fig. 4, shaded bars in panel A).

All *janus* singlets are characterized by invariant formation of oral primordia along the *pOM* and unreliable oral development along the *sOM*. A cell with oral structures along the *sOM* that is undergoing oral development may have an sOA without an sOP or, conversely, an sOP without an sOA. However, the likelihood of development of an sOP is higher if an sOA is present than if one is absent (Jerka-Dziadosz & Frankel, 1979, fig. 7). These same features of development of sOPs were observed both in doublets and derived singlets in this study (data not shown). This implies that even when a secondary oral area was absent from a semicell of a *janus* doublet, the capacity to generate new secondary oral structures was retained (Figs 10, 15). Development of primary oral structures was also not completely reliable in *janus* doublets: one case was seen of a developing cell with no oral primordium along one of

the two *pOM*s and two cases were observed with primary oral primordia but no corresponding primary OAs. This indicates that the potential for a *pOM* may occasionally persist despite the absence of primary oral structures at that site. [This corresponds to the

'monostome doublet' condition reported by Nanney (1966a). One derived singlet with an unusually high corticotype and aberrant cytogeometry was judged as likely to possess such a 'cryptic' second *pOM* and was therefore excluded from the statistical analysis in
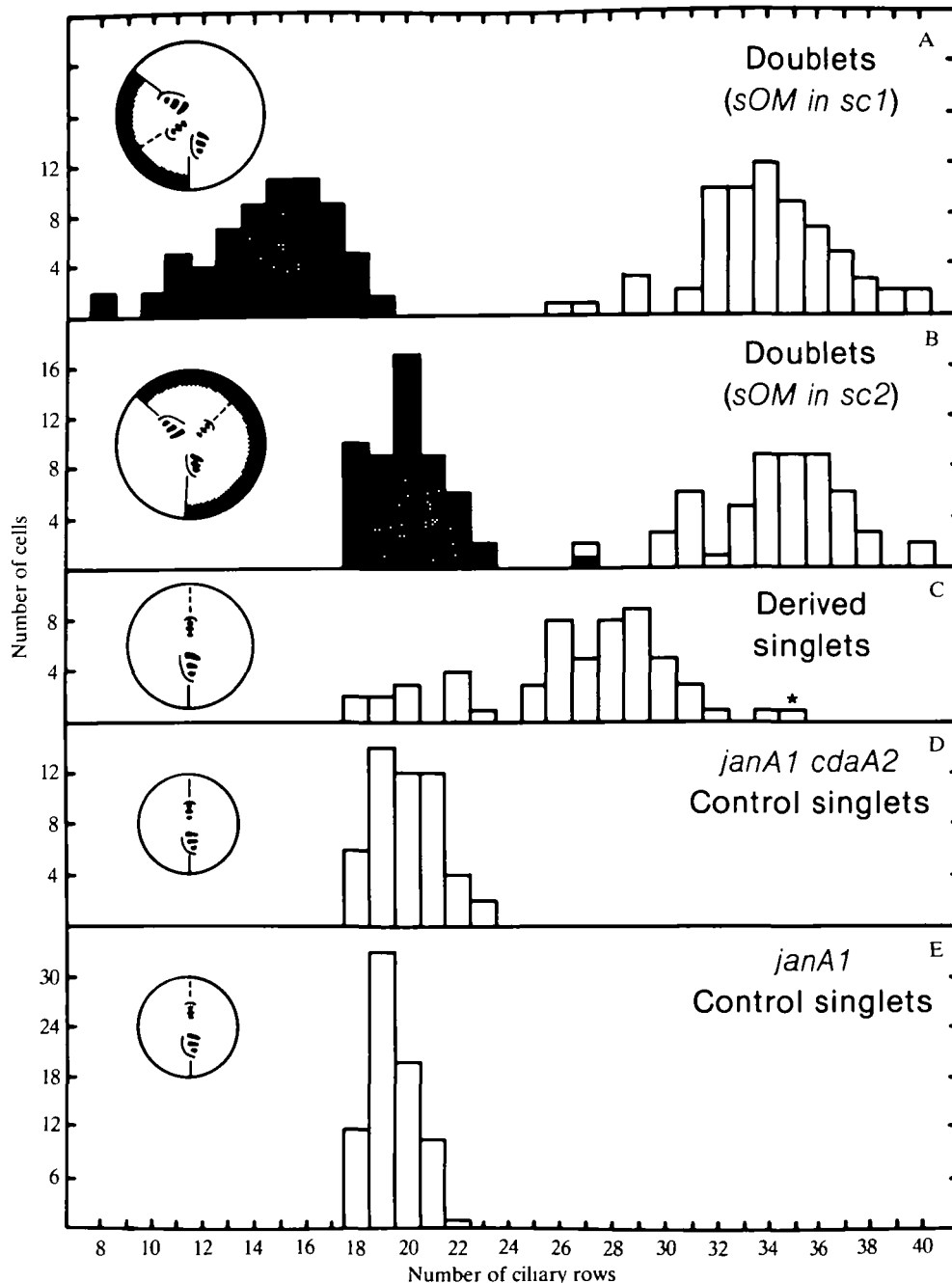


Fig. 4. Bar graphs illustrating the total number of ciliary rows (open bars) and the number of ciliary rows in semicell 1 (shaded bars in A) or in semicell 2 (shaded bars in B) of: doublets of stock IA207 clone no. 7 with an *sOM* in *sc1* (A) or with an *sOM* in *sc2* (B), and of singlets (with an *sOM*) derived from doublets of stock IA207 clone no. 7 (C), control singlets of stock IA207 (D), and control singlets of stock IA203 (E). Since 22 of the 99 doublets of panels A and B have *sOM*s in both *sc1* and *sc2* (the illustrative diagrams show doublets with sOAs in one semicell only), the data sets represented by the open bars of panels A and B are partially redundant. The data are based on tallies of (A) 67 semicells, (B) 54 semicells, (C) 56 cells, (D) 50 cells and (E) 77 cells. In this Figure and in Figs 18 and 19, the vertical scale is more compressed in E than in the other panels, in approximate proportion to the larger sample size in E. The starred bar indicates a probable 'monostome doublet' (see text).
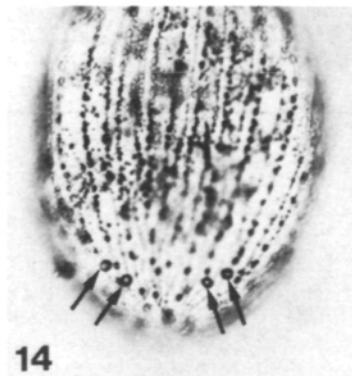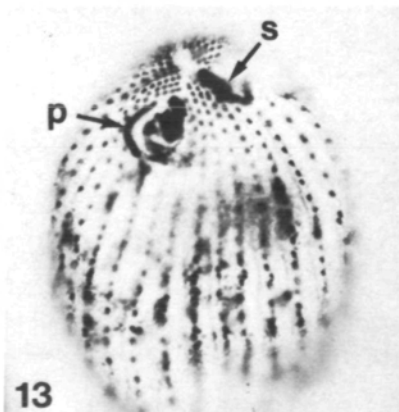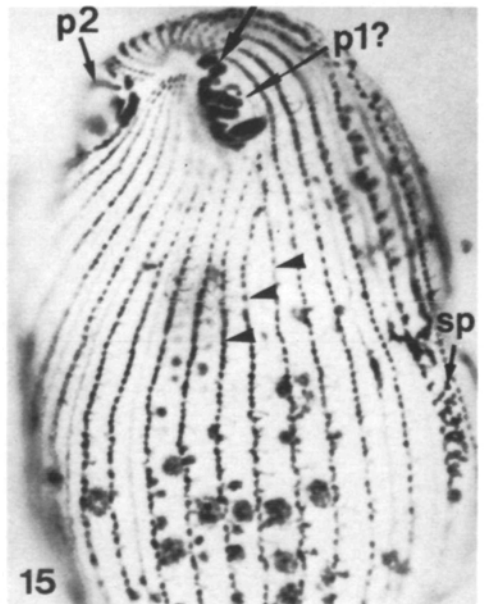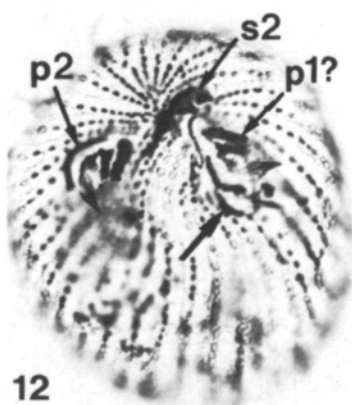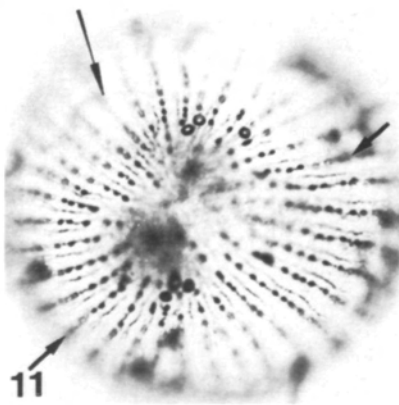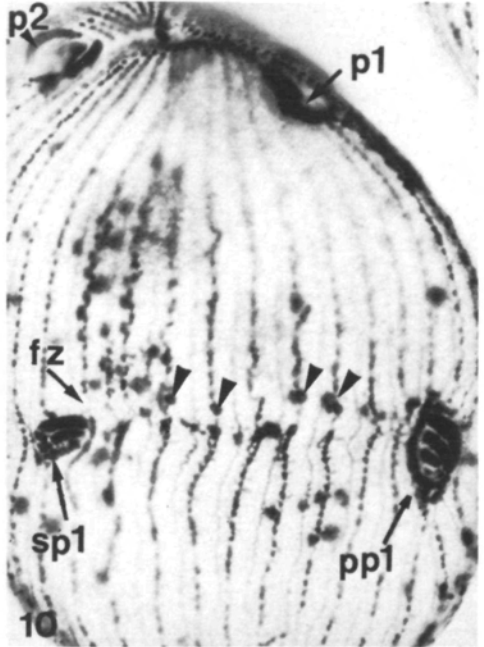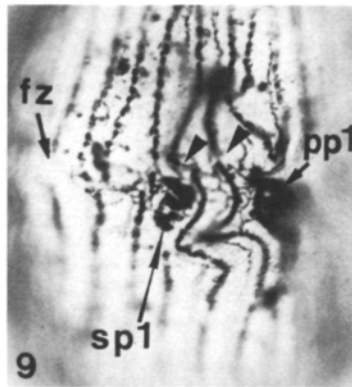
Table 1, though included in Figs 4, 18 and 19 (bars marked with asterisks)].

### (3) Contractile vacuole pore cytogeometry

In a *janus* singlet, CVPs are always located in *sr1*, to the right of the *pOM* and to the left of the *sOM* (Fig. 3C). The CVP arc is often interrupted by one or more ciliary rows that lack CVPs,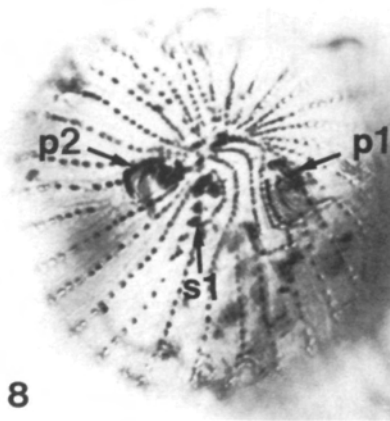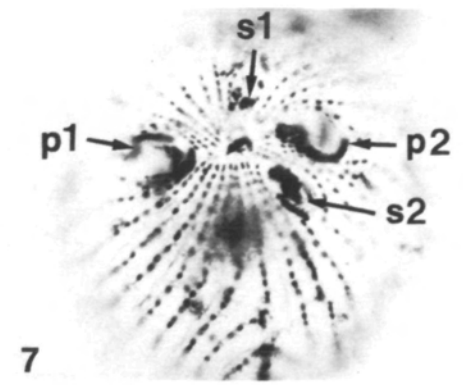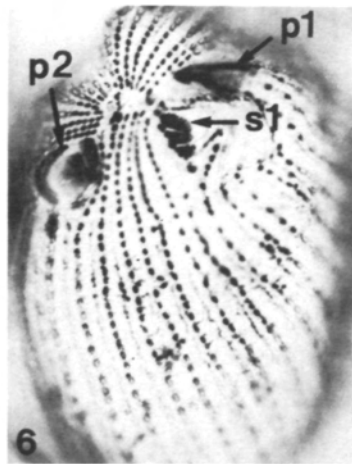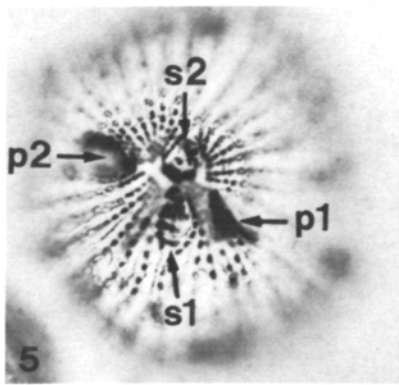 producing a gap within the CVP set. This can be thought of as dividing the set into two subsets, one to the right of the *pOM* and one to the left of the *sOM* (see Jerka-Dziadosz &

Frankel, 1979). While the total number of ciliary rows bearing CVPs can be as many as five, there is always only one gap, which is usually centrally located within the CVP arc (Frankel & Nelsen, 1981, 1986*b*). These characteristics of the CVP set are independent of whether or not secondary oral structures are actually present, suggesting that in established *janus* clones the CVP cytogeometry is not strongly dependent upon the actual expression of secondary oral structures (Jerka-Dziadosz & Frankel, 1979; Frankel & Nelsen, 1981).

---

**Figs 5–15.** Silver-impregnated *Tetrahymena thermophila* doublets and derived singlets from heat-treated clones no. 7 and no. 10 of stock IA207. The positions given in the legends all are numbered with reference to the right postoral row of pOA1, which is designated as row no. 1. Photographs are printed either in polar or lateral views, in the latter case with the anterior end of the cell at the top, and the cell's left corresponding to the viewer's right. ×1100.

**Fig. 5.** An anterior polar view of a slightly unbalanced 37-rowed doublet from clone no. 7, with two pOAs (p1, p2) and two sOAs (s1, s2). The two pOAs, both beneath the plane of focus, are located at rows 1 and 18, while the sOAs are located at rows 9 and 29, close to the centre of their respective semicells.

**Fig. 6.** An oblique anterior–polar view of a nearly balanced 38-rowed doublet from clone no. 7. The two pOAs (p1, p2) are located at rows 1 and 19, and there is a single rather well-developed sOA (s1) at row 11, near the middle of *sc1*. The pattern of anterior terminations of the ciliary rows to the right of an sOA is clearly visible in this photograph (for s1) and in the next one (for s2), and resembles that found to the left of a pOA (see Frankel *et al.* 1984).

**Fig. 7.** An anterior polar view of a slightly unbalanced 35-rowed doublet from clone no. 7. The two pOAs (p1, p2) are located at rows 1 and 17 (notice that in this case *sc1* is at the top of the picture). The sOA1 (s1), at row 10, is rudimentary, while the sOA2 (s2), at row 23, is well-developed. In this case, unlike Fig. 5, the sOAs (especially sOA2) are not at the centre of their respective semicells.

**Fig. 8.** An anterior polar view of a highly unbalanced 30-rowed doublet from clone no. 10. The pOAs (p1, p2) are at rows 1 and 11, while the single sOA (s1) is at row 6, the centre of *sc1*.

**Fig. 9.** A part of the ventral surface of an unbalanced 32-rowed doublet from clone no. 10, showing stage-5 oral primordia just posterior to the fission zone (fz). In this cell, the two pOAs (not shown in the photograph) are located at rows 1 and 15, and there are no sOAs. The pOP1 (pp1) is partially out of focus, while the sOP1 (sp1) is located at row 4, very close to the pOP1. No new CVPs are developing at the expected locations (arrowheads) within *sr11*.

**Fig. 10.** A view of part of the ventral surface of a nearly balanced 40-rowed doublet of clone no. 7, showing

stage-5 oral primordia just posterior to the fission zone (fz). The two pOAs (p1, p2) are located at rows 1 and 19, and there are no sOAs. A well-developed sOP1 (sp1) is located at row 10, in the middle of *sc1*. The membranelles of the sOP1 are tilted in a direction opposite to those of the pOP1 (pp1), a common feature of secondary oral primordia (Frankel *et al.* 1984). Four new CVPs (arrowheads) are developing just anterior to the fission zone within *sr11*.

**Fig. 11.** A posterior polar view of a moderately unbalanced 35-rowed doublet of clone no. 7. The two pOAs (out of focus at the opposite end of the cell; right-postoral meridians indicated by short arrows) are located at rows 1 and 16, while a single sOA is located in *sc2* at row 26 (postoral meridian marked by a long arrow). There are two sets of CVPs (unlabelled), one within *sc1* at rows 4, 5 and 6, and the other within *sc2* at rows 19, 22 and 23.

**Fig. 12.** An anterior polar view of an unbalanced 34-rowed doublet from clone no. 10. There is one clear-cut pOA2 (p2), and one sOA (s2) in *sc2*. The oral apparatus at the location expected for the pOA1 (p1?) has an extra posterior portion of the UM (arrow) including an associated deep fibre.

**Fig. 13.** A ventral view of a highly unbalanced 29-rowed derived singlet from clone no. 7 with the pOA (p) in focus. The sOA (s), partially out of focus, is located at row 21.

**Fig. 14.** A view of the posterior portion of *sr1* of a highly unbalanced 27-rowed derived singlet from clone no. 7. The sOA (not shown) is at row 17. The CVPs (arrows) are located at rows 5, 6, 12 and 13, separated by five rows that lack CVPs.

**Fig. 15.** A ventral view of an unbalanced 30-rowed doublet from clone no. 7. There is one clear-cut pOA2 (p2) on the left side of the photograph, and no typical sOA. The OA at the location expected for pOA1 (p1?) is highly abnormal, with a smaller supernumerary set of membranelles (arrow) located anterior to the more typically located set, and three postoral ciliary rows (arrowheads) instead of the two rows typical for a pOA or the one row characteristic of an sOA. A stage-1 sOP (sp) is seen at the right side of the photograph; a similar pOP (not shown in the photograph) is present posterior to pOA2, but there is clearly no OP posterior to the abnormal compound OA.

These characteristics of CVP sets were also manifested by the majority of *janus* doublets and derived singlets observed in this study. In doublets, when secondary oral structures were present within a semicell, the CVPs were always found in an *srl*; when secondary oral structures were absent, CVPs were found at an equivalent relative location within the semicell. Gaps were usually present within CVP sets, especially in the wider sectors (Fig. 11). There was only a single gap within each CVP set and the gap was usually centrally located (data not shown).

The array of cell surface phenotypes was similar in all clones, with differences only in the overall progression from the doublet to the singlet condition. Clone no. 10 had a relatively high proportion of severely unbalanced doublets; in view of our special interest in such cells (see below) we made a selective tally of unbalanced doublets in this clone.

### (B)  *How* janus *doublets reorganize into singlets*

#### (1)  *General considerations*

The way in which *janus* doublet cells reorganize to singlets allows us to distinguish between the two alternative interpretations of the *janus* phenotypes set forth in the Introduction. We recall that if *janus* mutant *Tetrahymena* are analogous to *Drosophila* pattern mutants with autonomous expression, so that the positional information is the same in wild-type and *janus* cells, then *janus* cells must differ from wild-type cells in the interpretation of this information. In that event, wild-type cells must possess both a normal ventral oral meridian and some stable positional information that is interpreted as a dorsal oral meridian in *janus* cells. If this view is correct, then all homopolar doublet cells, both wild-type and *janus*, must possess the spatial information for four oral meridians, two of the ventral (primary) type and two of the dorsal (secondary) type. But then there is a difficulty in conceiving of what happens when a doublet reverts to a singlet. If pre-existing positional information is always conserved during clonal growth, then wild-type singlets derived from regulation of doublets must retain the spatial coordinates of all four oral meridians, three of which are not expressed; this supposes an implausible degree of hidden complexity. Alternatively, one can imagine that when wild-type or *janus* doublets regulate to the singlet state, one pair of oral meridians is truly lost while the other pair is conserved; this is more plausible but also suggests that intracellular positional information is itself subject to change. This leads us to attempt to account for both the difference between *janus* and wild-type cells and the regulation from the doublet to the singlet state in terms of a global positional system in which positional values can undergo rapid readjustment. In order to evaluate

this possibility in a specific and systematic manner, we have organized our observations around a global model that we have formulated earlier (Nelsen & Frankel, 1986; Frankel & Nelsen, 1986*a,b*). We will here summarize the model [originally inspired by the polar-coordinate model of French, Bryant & Bryant (1976)], and then use it to generate predictions for the reorganization of *janus* doublets into singlets. Most of the predictions are not derivable from, and often are irreconcilable with, the alternative idea of differential interpretation of unchanging positional information.

### (2)  *The intercalation model*

The model postulates a continuous positional system that is arrayed around the cell circumference. This system can be diagrammed by labelling positions around the cell circumference with numbers indicating different positional values (Fig. 16A), much as positions around the circumference of a traditional clock are labelled with numbers indicating different times. As in a clock, a numerical discontinuity (10/0 in Fig. 16A) must exist somewhere around the circle, but this numerical discontinuity is merely a topological consequence of numbering positions on a circle and thus is intrinsically no different from any other position around the circle. The positional values in turn determine the circumferential location of cell structures. Oral structures are arbitrarily assumed to be specified at the positional value of 5, while CVPs are specified in a zone centred at the value of 7. The direction of ordering of positional values determines the large-scale asymmetry of the oral structures and of the configuration of basal-body couplets at the apical crown of the cell (Frankel *et al.* 1984). The positional values are assumed to be propagated longitudinally during clonal growth and thus to maintain stability in the circumferential locations of the structures that they specify. This stability is compromised only when (a) the spacing of positional values deviates sufficiently from the normal, and/or (b) a sufficiently great discontinuity is created in the array of values.

Using this model, the effect of *janus* mutations is viewed as an incapacity to maintain a subset of (dorsal) positional values, which triggers replacement of this subset by the complementary subset arrayed in a reversed order. Here we assume that the range of values 8-9-10/0-1-2 is dependent on a putative *janA*[+] gene product for its maintenance. As *janA*[+] gene product is diluted out following the substitution of *janA1* for *janA*[+], there would be an ever-increasing dorsal discontinuity coupled with a simultaneously increasing spreading out of the remaining positional values (Fig. 16B,C). When a critical discontinuity and/or degree of expansion of remaining values is reached (Fig. 16C), the system would undergo a
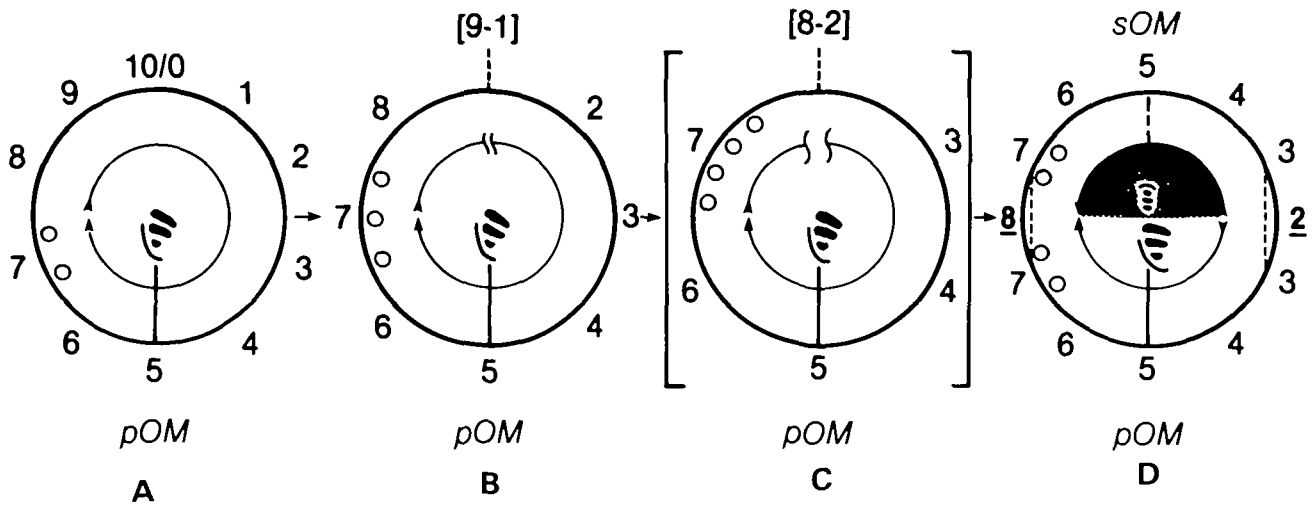
**Fig. 16.** An intercalation model for the expression of the *janus* phenotype. The diagrams are highly schematic polar projections, showing OAs, CVPs, *pOM*s (solid radii) and *sOM*s (dashed radii). The outer circle is labelled with putative positional values, and the primary oral meridian (*pOM*) and secondary oral meridian (*sOM*) are indicated. The inner circle indicates the global ordering of these positional values. In the inner circle, the arrow heads and tails indicate the direction of asymmetry resulting from this global ordering, while ∫∫ represents a discontinuity in the sequence of positional values. The normal situation with one complete set of positional values is indicated in A, an intermediate condition of loss of some dorsal values (from 9 to 1) in B, a greater extent of loss (8 to 2) in C, and the result of reversed intercalation in D. Diagram C is bracketed to indicate that it is an unstable intermediate configuration. In diagram D, the numbers representing longitudes of symmetry are in bold face underlined and the region of reversed global asymmetry is shaded in the inner circle. The dashed vertical chords near positions 8 and 2 in D indicate potential sites of local elimination of positional values by intercalation across lines of symmetry. Slightly modified from Frankel & Nelsen, 1986*b*.

massive reorganization that would restore continuity and near-normal spacing by the only means possible, which is reverse intercalation. The 8/2 discontinuity would thus be replaced by the sequence 8-*7-6-5-4-3*-2 (intercalated values italicized). This reorganization would generate a second oral meridian with reversed large-scale asymmetry (Fig. 16D).

In this model, there is no fundamental reason for assuming that the position of the newly generated *sOM* relative to the *pOM* is fixed. The same reorganization that creates the *sOM* also generates two lines of symmetry in the configuration of positional values (at the values 8 and 2 in Fig. 16D). At both of these lines, further elimination of positional values could occur in a local, incremental manner (as shown by dashed chords in Fig. 16D). However, if established *janus* clones are near the corticotypic 'stability centre' (Nanney, 1966*a,b*; Frankel, 1980), the spacing of positional values in relation to the ciliary rows should be near its optimal value. There would then be little change in positional value at the lines of symmetry and hence little variation in the relative positions of the *pOM* and *sOM*. Stability in relative location of oral structures is indeed characteristic of established *janus* clones (Jerka-Dziadosz & Frankel, 1979; Frankel & Nelsen, 1981, 1986*b*).

Doublets are initially far from the stability centre and lose ciliary rows as they regulate to singlets (Fig. 4). In non-*janus* doublets, where there are two complete sets of positional values in tandem array [topologically, with a 'winding number' (see Winfree, 1980, p. 14) of 2], positional values would become more crowded in one semicell as ciliary rows are lost and the positions of oral meridians undergo random slippage. Regulation to relieve this crowding must then involve a major reorganization with reversal in direction of positional values within one array (Nelsen & Frankel, 1986; Frankel & Nelsen, 1986*a*), leading to a temporary imitation of the *janus* condition (see section C). In *janus* doublets, in which the postulated reversal shown in Fig. 16 would have already been accomplished when the *janus* mutation had come to expression, the initial positional organization would be altogether different from that of non-*janus* doublets: there would be four domains of symmetrical subsets of positional values, one in each sector, with lines of mirror symmetry in the middle of each sector (Fig. 17A). As the number of ciliary rows decreased, positional values could be lost by incremental intercalation across any of the four lines of symmetry, potentially leading to loss of a whole sector. When two adjacent sectors become lost by this

means, the *janus* doublet of Fig. 17A would be converted to the *janus* singlet of Fig. 17J.

The positional organization postulated for *janus* doublets virtually precludes any catastrophic reorganization of the underlying positional system but predicts a dramatic morphological transformation. As a sector collapses, adjacent primary and secondary oral meridians must approach one another, merge and then disappear. There are two ways in which this can occur, either across an *sr2* with fusion of an *sOM* with the *pOM* to its right (Fig. 17, top), or across an *sr1* with fusion of an *sOM* with the *pOM* to its left (Fig. 17, bottom). In either case, reorganization should progress through three phases: first (phase I) convergence of oral meridians as successive positional values are incrementally lost at the symmetry line (Fig. 17B–C or F–G); then (phase II) fusion of two oral meridians quickly followed by their loss as the positional value of the symmetry plane either rises above 5 (Fig. 17D) or falls below 5 (Fig. 17H) and the sector vanishes; finally (phase III) coalescence of positional values to eliminate positional redundancies within the merged sectors adjacent to the vanished sector (Fig. 17E or I).

While the two sequences described above are nonarbitrary consequences of the model, some of the details, particularly in the merger of the sectors complementary to the one that has vanished (e.g. of *sr21* with *sr22* after *sr11* has disappeared) can vary substantially, and are presented in an arbitrary manner in Fig. 17. The specific order of events presented in the figure is to some degree chosen *a posteriori* from our observations. However, the predictions to follow are virtually unaffected by this arbitrary aspect; they are basically *a priori* predictions derived from the intercalation model. They are not derivable from, and in large part not consistent with, a model with preformed propagated pattern boundaries, since such a model could permit disappearance of structures (due to altered expression or interpretation of 'prepatterns' or positional information) but could not accommodate the sequence of mutual approach, merger and loss that derives naturally from the intercalation model.

### (3) Predictions of the intercalation model

There are distinctive predictions for each phase of regulation.

The predictions for phase I (convergence) are:

**1.** The variance in relative location of secondary oral structures should be high, especially in the narrower semicell (*sc1*) in which sector collapse is



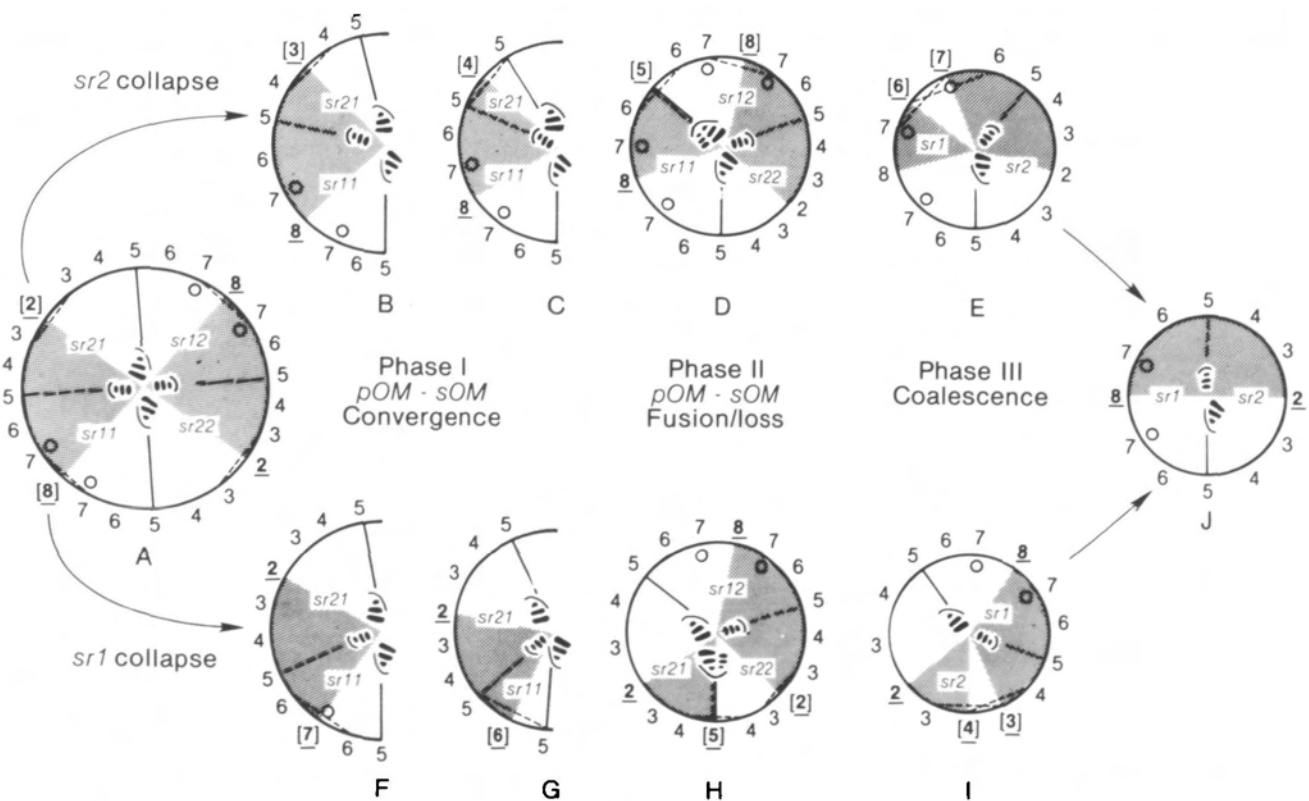**Fig. 17.** The intercalation model applied to the transformation of *janus* doublets (left) to *janus* singlets (right). The illustrative conventions are those of Fig. 16, simplified by representing adjacent CVPs with single large circles, and by omission of the inner circle. Sectors are labelled. The bracketed positional values are those that are being eliminated. For further explanation, see the text.

occurring. This high variance should come about because different cells in a culture should be in different stages of sector collapse and because collapse might occur across either sector.

2. Although the CVP midpoint should always be near the middle of its sector (*srl1* or *srl2*), its position within the semicell should be highly variable because of the great variation in the relative widths of the two sectors. [The central location of *CM1* within *srl* is expected due to the symmetrical organization of positional values within sectors, but is also predicted by the earlier model, which postulates overlapping gradients symmetrically organized with reference to fixed boundaries (Frankel & Nelsen, 1981, 1986*b*)].

3. As an *srl* (presumably *srl1*) becomes narrower (Fig. 17, bottom sequence), the CVP arc also should get narrower. CVPs should be altogether absent from the narrowest sectors. This is an especially strong prediction since it is *not* compatible with any simple version of the alternative model mentioned above.

There is one obvious and critical prediction for phase II (fusion/loss):

4. Close approaches and actual fusions of *sOM*s and *pOM*s should be observed, with CVP configurations as shown in Fig. 17D,H.

There are three predictions for phase III (coalescence):

5. The relative location of the *sOM* within the cell circumference should be more variable in *janus* singlets recently derived from doublets than in *janus* singlets that had not recently been through the doublet condition. This difference in variance is expected because different derived singlets will be in different stages of incremental loss of symmetrically redundant positional values (Fig. 17E,I).

6. For the same reason, the relative location of the CVP midpoint within the whole cell (but not within *srl*) should be more variable in derived *janus* singlets than in steady-state singlets.

7. If initial collapse had occurred in an *sr2* (presumably *sr21*) (Fig. 17, upper sequence), some derived singlets should have three, or even four, groups of contiguous CVP rows separated by ciliary rows without CVPs (Fig. 17E).

Testing these predictions requires comparing *janA1/cdaA2* doublets and derived singlets with otherwise equivalent *janus* cells that have not passed through the doublet state. This entails a double comparison: first, a comparison of *janA1/janA1 cdaA2/cdaA2* (clone IA207) cells with *janA1/janA1 cdaA2⁺/cdaA2⁺* (clone IA203) cells to find out whether *cdaA2* has any interactive effect on *janus* cytogeometry, and second, a comparison of the cytogeometry of cells of the heat-shocked IA207 clones with non-heat-shocked *janus* cells of the same and related clones. While the first comparison was

conducted within the same experiment, the second one was not: the 'experimental' cells were exposed to 39°C, cloned and then grown in tubes at 30°C, whereas the 'control' cells were not heat treated, not recloned, and were grown in flasks at 28°C (see Materials and Methods). These differences, however, do not vitiate the comparison: prolonged exposure to 39°C has no effect on the expression or cytogeometry of *janA1* cells (Jerka-Dziadosz & Frankel, 1979; Frankel, unpublished data) and the cytogeometrical parameters of *janus* cells do not show a high clonal fidelity (Frankel & Nelsen, 1981). To the extent that cloning of the 'experimentals' might bias the comparison, the bias opposes our predictions, since recent clonal origin should reduce variance, whereas our predictions call for *increase* in variance.

### (4) *Tests of the predictions*

A condition for testing the above predictions is that the controls be of reasonably uniform cytogeometry. Such uniformity was indeed observed, both in the IA207 and IA203 cells used as specific controls for this study (Table 1; panels D and E in Figs 4, 18, 19) and in *janus* stocks in general (not shown).

1. *Variance in location of secondary oral structures of* janus *doublets.* The prediction of great variation in relative location of secondary oral structures in *janus* doublets, especially within the narrower semicells, is confirmed (Fig. 18; Table 1; Figs 5–10). The coefficient of variation (c.v., standard deviation divided by the mean) of the relative location of *sOM1* in *sc1* is triple that of control *janus* singlets, and the c.v. of the relative location of *sOM2* in *sc2* is double that of control *janus* singlets (Table 1, column 1).

The relative position of *sOM1* within *sc1* (in clone no. 7) showed a weak ($r = 0.36$) but significant ($P < 0.01$) positive correlation with the width of the semicell. In semicells with 15 row-intervals or more, the secondary oral structures were located, on the average, near the centre of the semicell, whereas in very narrow semicells (14 row-intervals or less), the mean relative position of *sOM1* was near 0.4, thus closer to *pOM1* than to *pOM2*. In the special sample of narrow semicells in clone no. 10 (semicell widths of 8 to 14), the mean relative position of *sOM1* was $0.347 \pm 0.104$ (n = 16). This leftward trend in the relative location of *sOM1* as *sc1* becomes narrower suggests that regulation occurs predominantly by collapse of *srl1* (Fig. 17, bottom sequence).

2. *Variance in location of CVP sets of* janus *doublets.* The prediction of unusually great variation in the relative location of CVP sets within semicells (but *not* sectors) of doublets is only weakly confirmed (Table 1). The major difficulty is that, unlike the

**Table 1.** *Variability of relational measures of positioning of secondary oral structures and of contractile vacuole pores*

| Type of cell | (1) Relative position of secondary oral structures ($srl/sc$ or $srl/c$) | | | | Relative position of the CM in | | | | | | |
| | | | | | (2) Sector ($d/srl$) | | | (3) Semicell ($d/sc$) | | | |
| | mean | S.D.* | C.V.* | n | mean | S.D. | C.V. | mean | S.D. | C.V. | n |
|---|---|---|---|---|---|---|---|---|---|---|---|
| *Doublet*† | | | | | | | | | | | |
| sOM in scl | 0·488 | ±0·083 | 17·0% | 67 | 0·513 | ±0·080 | 15·5% | 0·265 | ±0·053 | 19·9% | 33 |
| sOM in sc2 | 0·510 | ±0·057 | 11·2% | 54 | 0·494 | ±0·075 | 15·3% | 0·249 | ±0·044 | 17·6% | 40 |
| *Derived singlet*† | 0·514 | ±0·064 | 12·4% | 55 | 0·487 | ±0·053 | 10·9% | 0·250 | ±0·039 | 15·7% | 55 |
| *Singlet* | | | | | | | | | | | |
| IA207 | 0·455 | ±0·026 | 5·7% | 50 | 0·509 | ±0·057 | 11·2% | 0·232 | ±0·026 | 11·1% | 50 |
| IA203 | 0·479 | ±0·026 | 5·5% | 77 | 0·479 | ±0·051 | 10·7% | 0·229 | ±0·024 | 10·4% | 77 |

* S.D., standard deviation; c.v., coefficient of variation.
† Doublet, doublets from stock IA207; Derived singlet, singlets derived from doublets of stock IA207.

situation for oral meridians, the 'background' variation for relative location of CVP midpoints (*CM*) within sectors is high. While the *average* relative CVP midpoints within sectors ($d/sr$), always near 0·5 (Table 1; Fig. 19), are in agreement with prediction, the c.v.s of the relative CVP midpoints are near 10 % in control *janus* singlets and are unexpectedly increased by one-half in the semicells of *janus* doublets (Table 1, column 2). The fact that variation in position of CVPs relative to OAs is intrinsically greater than variation in position of OAs relative to each other may be due, in part at least, to the fact that a given cell's CVPs and OAs are formed in different cell generations, so that the locations of CVPs may not accurately reflect the current positions of the oral meridians (Frankel & Nelsen, 1986b).

If prediction 2 is correct, then the c.v. of the relative CVP midpoint must be greater when judged relative to the width of the semicell containing the CVP ($d1/scl$ or $d2/sc2$) than when judged relative to width of the sector in which the CVP set is located ($d1/srl1$ or $d2/srl2$), and the semicell *versus* sector difference should be increased in the semicells of *janus* doublets, particularly in the narrower semicells ($scl$). The relevant differences, obtained by subtracting the c.v. values of column 2 of Table 1 from the corresponding values of column 3, are consistent with this prediction, but are not very large.

**3.** *Loss of CVPs from narrowest sectors.* The predictions that CVP arcs should become narrower as the width of an *srl* (*srl1* or *srl2*) decreases and that CVPs should disappear from the narrowest sectors are strongly confirmed (Fig. 20). Examples of two extreme sector widths are illustrated in Figs 9,10. The results of the detailed survey of clone no. 7 (Fig. 20, open symbols) and the special tally of narrow sectors in clone no. 10 (Fig. 20, closed symbols) are mutually

compatible (the numbers in parentheses in Fig. 20 will be considered in section C).

**4.** *Fusions of* sOMs *and* pOMs. The prediction of close approaches and fusions of secondary and primary oral meridians has been confirmed for fusion of an *sOM* with a *pOM* on its *left* (as in Fig. 17H), but not for fusion of an *sOM* with a *pOM* on its *right* (as in Fig. 17D). Several secondary oral structures were observed at three-row intervals to the right of corresponding primary oral structures (Fig. 9), two were seen at two-row intervals and none were found at a one-row interval. The latter probably signifies that adjacent oral primordia frequently fuse as they develop (E. Cole, personal communication). Configurations suggestive of fusions between sOAs and pOAs have been observed in several cells; two examples are shown in Figs 12 and 15. In Fig. 12 there is an unmistakable supernumerary UM fragment to the posterior right of the UM of an otherwise normal OA, whereas in Fig. 15 the presumed fusion OA possesses two sets of membranelles and three postoral ciliary rows instead of the normal two. The overall configuration of these cells is that shown in Fig. 17H: in addition to the putative fusion OA, a normal OA is present in the location expected for a pOA2 (labelled p2, Figs 12, 15), and an sOA (s2, Fig. 12) or an sOP (sp, Fig. 15) is present in *sc2*; CVPs (out of the focal plane in the photographs) are located in the positions shown in Fig. 17H. If the putative fusion OA were absent, the result in both cases would be a *janus* singlet with a single sOA almost directly opposite the pOA. The cell shown in Fig. 15 appears to have been in the process of undergoing this transformation, since it has a stage-1 oral primordium at the *sOM2* position (sp) and
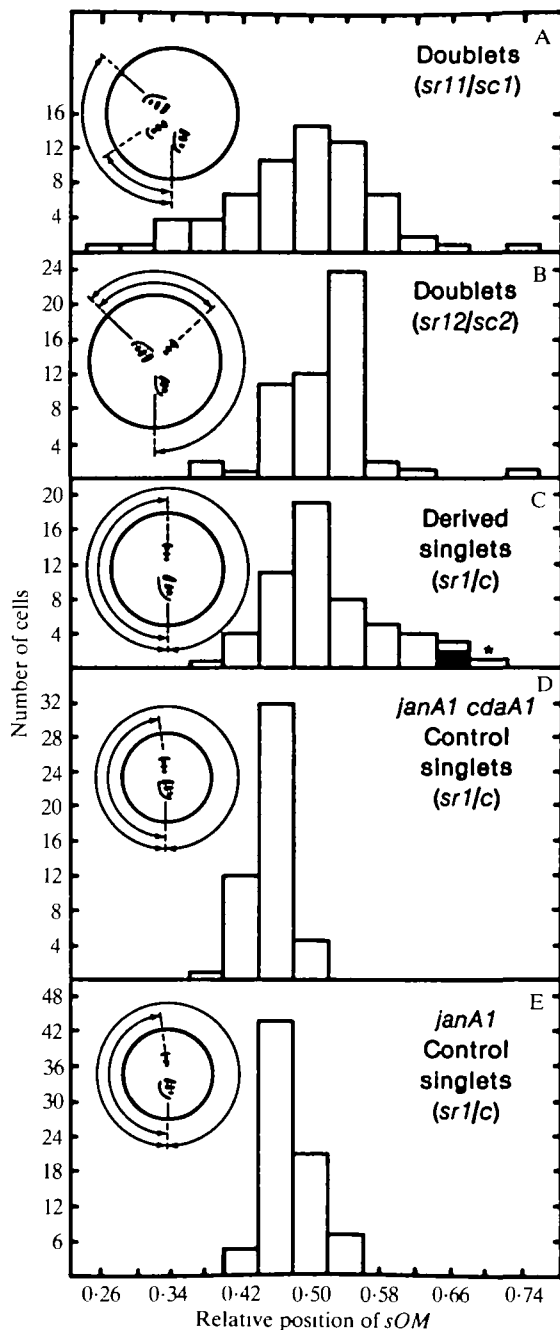
**Fig. 18.** Bar graphs indicating the relative position of the secondary OA in the semicell (A,B) or whole cell (C,D,E) of the same sets of cells as in Fig. 4. The shaded bar represents two cells with three separate CVP subsets, while the bar with the asterisk indicates the one aberrant 'monostome doublet'. The accompanying diagrams illustrate the features under consideration, in the same style as Fig. 3.



**Fig. 19.** Bar graphs indicating the relative position of the CVP midpoint within *sr1*. The five panels correspond to those of Fig. 18, and the shading and asterisk represent the same cells as are correspondingly marked in Fig. 18. For panels C,D and E the samples are identical to those plotted in Fig. 18, while for panels A and B they are the subsets (of 33 and 40, respectively) that possessed CVPs and were scorable for CVP as well as oral positions. The accompanying diagrams illustrate the features under consideration.

another oral primordium posterior to the normal OA (p2) at the *pOM2* position (not shown in photograph), but has no oral primordium posterior to the fusion OA (p1?). If this cell had been allowed to divide, the posterior division product would have
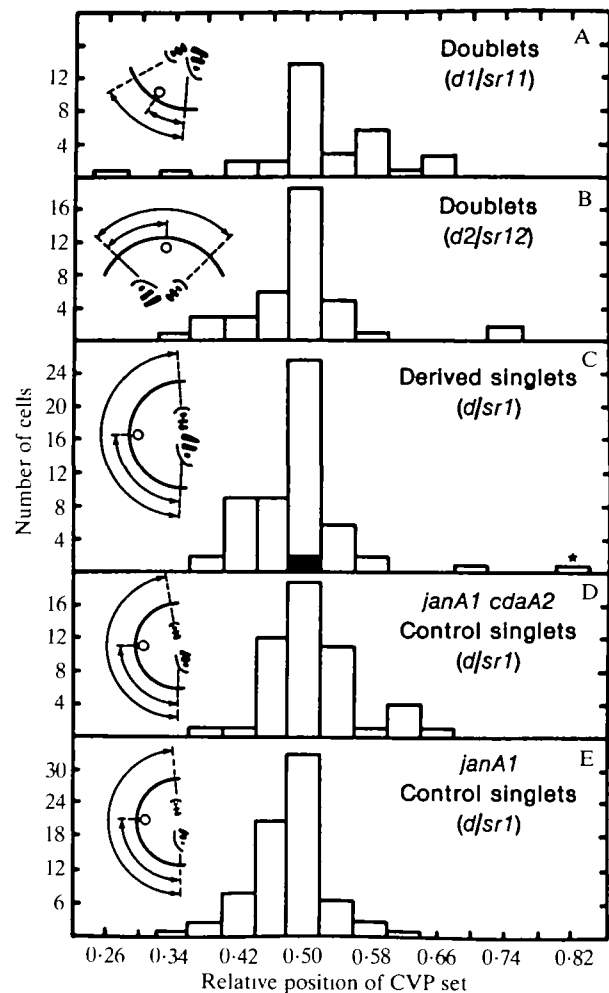
been a *janus* singlet, with no OA along the fusion meridian.

The closest approach seen of a secondary oral structure to a primary oral structure on its *right* was four-row intervals (seen once); distances of five-row intervals (Fig. 8) were observed a few times. There were no cases clearly corresponding to Fig. 17D. Thus direct evidence is lacking for completion of the postulated collapse of an *sr2* (Fig. 17, top sequence).

**5.** *Variance in location of secondary oral structures of derived* janus *singlets.* The prediction that the variation in the relative position of the *sOM* of *janus* singlets derived from doublets is greater than that in
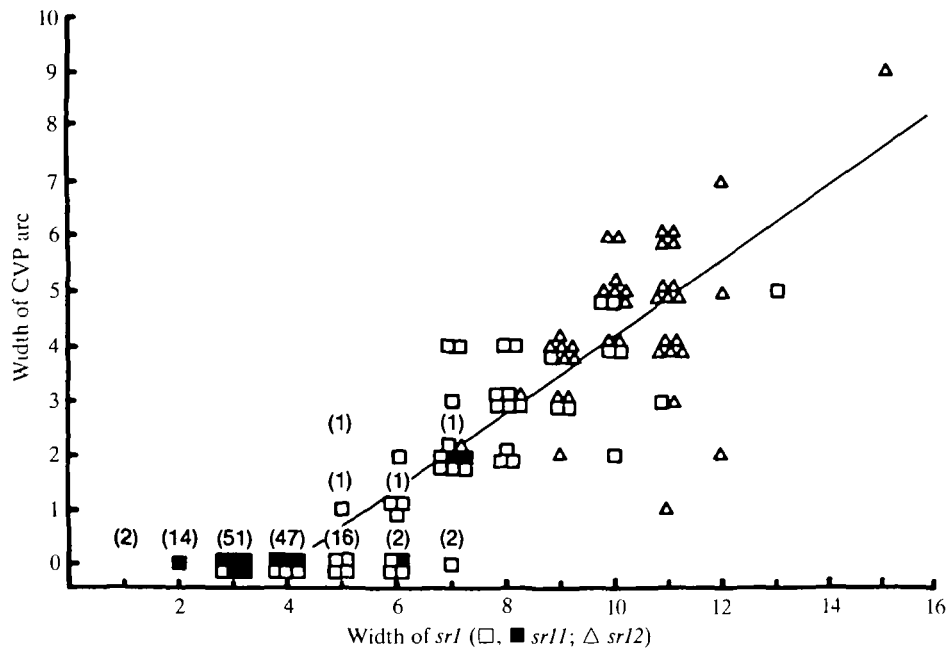
**Fig. 20.** Width of the CVP arc (ordinate) plotted against width of *sr1* (abscissa) in doublets that possess *sOM*s. A width of zero on the ordinate indicates absence of CVPs in *sr1*. Squares represent semicells with the *sOM* in *sc1*, in IA207 clone no. 7 (open) or clone no. 10 (shaded), while triangles represent semicells of clone no. 7 with the *sOM* in *sc2*. The numbers in parenthesis summarize separate data for CVPs in *sc1* of unbalanced non-*janus* doublets from the study of Nelsen & Frankel (1986). The line gives the least-squares linear regression computed for all of the data from IA207 clone no. 7 (open symbols).

ordinary *janus* singlets is confirmed. The evidence is summarized in Table 1 and Fig. 18. When compared with ordinary *janus* singlets (Fig. 18D,E), the most striking imbalances involve an *sr1* larger than the *sr2* (Fig. 18C; an example is shown in Fig. 13). Such cases correspond more closely to the geometry expected from collapse of an *sr2* (Fig. 17E) than with that derived from collapse of an *sr1* (Fig. 17I).

**6. Variance in location of CVP sets of derived** janus *singlets*. The prediction that the variance of the relative position of the CVP set is greater in *janus* singlets derived from doublets than in typical *janus* singlets is weakly supported by the results (Table 1); the problems here are the same as for the corresponding prediction 2 for doublets.

**7. Multiple CVP subsets in derived** janus *singlets*. The prediction of three subsets of contiguous CVP rows has been confirmed in two cells. Both of these cases also involve a major imbalance of the two sectors, with *sr1* twice as wide as *sr2* (Fig. 18C). The cytogeometry of OAs and CVPs in these two cells corresponds to that diagrammed in Fig. 17E.

An unanticipated observation was the large separation between two CVP subsets that was sometimes observed in wide sectors of unbalanced derived singlets (Fig. 14). Similar widely spaced CVP subsets

were occasionally observed in *sr12* of highly unbalanced doublets; these were presumably forerunners of the corresponding situation in some derived singlets. This wide separation is probably associated with a transition from the doublet-to-singlet state at an unusually high corticotype (see section A2), so that a single sector may contain as many ciliary rows as an entire normal cell.

In summary, predictions 1, 3, 4, 5 and 7 are clearly confirmed, while predictions 2 and 6 are less strongly supported. The evidence relating to phases I and II (especially predictions 1 and 4) strongly suggest collapse of *sr11* (Fig. 17, bottom sequence), while the evidence relating to phase III (especially predictions 5 and 7) suggest collapse of *sr21* (Fig. 17, top sequence). In many highly unbalanced doublets, both *sr11* and *sr21* simultaneously become quite narrow. It is possible that this results in a global instability that somehow brings about a rapid loss of an *sOM* plus either of the two adjacent *pOM*s without actual prior fusion of complementary oral meridians.

(C) *A comparison of reorganization of* janus *and* non-janus *doublets*

We have recently observed that reorganization of non-*janus* doublets into singlets often involves transient formation of a secondary OA in the narrower semicell, with simultaneous disappearance of CVPs

from that same semicell (Nelsen & Frankel, 1986). A comparison of the reorganization of *janus* and non-*janus* doublets into singlets reveals one major difference and one important similarity. The difference is that in *janus* doublets secondary oral structures were formed with equal frequency in the narrower and wider semicells of unbalanced doublets, whereas in non-*janus* doublets such structures appeared only in the narrower semicell, and then only when the width of that semicell was 14 ciliary row-intervals or less (usually 12 or less). The similarity is that within such narrow semicells the cytogeometry of the *sOA* and the CVP sets was indistinguishable in *janus* and non-*janus* cells: in both classes, the position of the secondary oral structures could vary widely but was typically closer to *pOM1* than to *pOM2*, and a CVP set was usually missing from *srl1* (Fig. 20). This similarity can be appreciated by comparing Fig. 8 of this paper to figs 3–6 of Nelsen & Frankel, 1986. Furthermore, corresponding cases of putative fusions of sOAs with pOAs to their left was obtained in both *janus* and non-*janus* doublets (compare Fig. 15 of this paper to fig. 8 of Nelsen & Frankel, 1986).

Both the difference and the similarity can be accounted for by the intercalation model. According to this model, the difference is due to the very different starting organization of the positional systems of non-*janus* and *janus* doublets: non-*janus* doublets have two complete sets of positional values organized in tandem around the cell circumference, permitting formation of a secondary OA only after the occurrence of reverse intercalation, an event that is possible only in the narrower semicell of unbalanced doublets (see fig. 19 in Nelsen & Frankel, 1986); by contrast, *janus* doublets are in the mirror-image state in both semicells from the start. The similarity is explained by the postulate that the positional organization that was achieved *after* reverse intercalation in the narrower semicell of the non-*janus* doublet was identical to that which was present from the start in both semicells of *janus* doublets. Regulating non-*janus* doublets in which secondary oral structures transiently appear in a narrow semicell can thus be thought of as unilateral phenocopies of *janus* doublets.

## Conclusions

1. Observations on the mode of regulation of *janus* doublets into singlets are clearly inconsistent both with the general idea of fixed pattern boundaries that are variably expressed by *janus* cells and also with a specific double-gradient model (Frankel & Nelsen, 1981, 1986*b*) that includes such fixed pattern boundaries as an important component. Instead, the observations for the most part confirm predictions made

from a model in which *janus* mutations interfere with the maintenance of a discrete subset of positional values, so that the *janus* phenotype is achieved by a reverse intercalation of remaining, permitted values across the territory normally occupied by the forbidden values. The *janus* mutations thus probably affect the positional system in a manner that is *not* locally autonomous. This makes it reasonable to infer that wild-type alleles at these loci are involved in maintaining the normal positional system.

2. The striking similarities in the way in which wild-type and *janus* cells regulate from the homopolar-doublet to the singlet state indicate that what is special about the *janus* condition is not a unique geometry but rather a unique long-term stability of that geometry. Reverse intercalation of positional values supplies a unifying interpretation for both the similarities and differences observed between *janus* and non-*janus* doublet cells: the similarities result from the stereotyped consequences of reverse intercalation, whereas the differences are due to the rather different circumstances required to provoke this type of reorganization.

## References

ANDERSON, K. & NÜSSLEIN-VOLHARD, C. (1986). The dorsal-group genes of *Drosophila*. In *Gametogenesis and the Early Embryo* (ed. J. Gall), pp. 177–194. New York: Academic Press.

FAURÉ-FREMIET, E. (1948). Doublets homopolaires et regulation morphogenetique chez le Cilié *Leucophrys patula*. *Archs Anat. microsc. Morph. exp.* **37**, 183–203.

FRANKEL, J. (1980). Propagation of cortical differences in *Tetrahymena*. *Genetics* **94**, 607–623.

FRANKEL, J. & HECKMANN, K. (1968). A simplified Chatton–Lwoff silver impregnation procedure for use in experimental studies with ciliates. *Trans. Am. microsc. Soc.* **87**, 317–321.

FRANKEL, J. & JENKINS, L. M. (1979). A mutant of *Tetrahymena thermophila* with a partial mirror-image duplication of cell surface pattern. *J. Embryol. exp. Morph.* **49**, 203–227.

FRANKEL, J., JENKINS, L. M. & BAKOWSKA, J. (1984). Selective mirror-image reversal of ciliary patterns in *Tetrahymena thermophila* homozygous for the *janus* mutation. *Wilhelm Roux Arch. devl Biol.* **194**, 107–120.

FRANKEL, J., JENKINS, L. M., DOERDER, F. P. & NELSEN, E. M. (1976). Mutations affecting cell division in *Tetrahymena pyriformis*. I. Selection and genetic analysis. *Genetics* **83**, 489–506.

FRANKEL, J. & NELSEN, E. M. (1981). Discontinuities and overlaps in patterning within single cells. *Phil. Trans. R. Soc. Lond.* B **295**, 525–538.

FRANKEL, J. & NELSEN, E. M. (1986a). Intracellular pattern reversal in *Tetrahymena thermophila*. II. Transient expression of a *janus* phenocopy in balanced doublets. *Devl Biol.* **114**, 72–86.

FRANKEL, J. & NELSEN, E. M. (1986b). How the mirror-image pattern specified by a *janus* mutation of *Tetrahymena thermophila* comes to expression. *Devl Genet.* **6**, 213–238.

FRENCH, V., BRYANT, P. J. & BRYANT, S. V. (1976). Pattern regulation in epimorphic fields. *Science* **193**, 969–981.

GERGEN, J. P. & WIESCHAUS, E. F. (1985). The localized requirements for a gene affecting segmentation in *Drosophila*: analysis of larvae mosaic for *runt*. *Devl Biol.* **109**, 321–335.

GERGEN, J. P. & WIESCHAUS, E. (1986). Localized requirements for gene activity in segmentation of *Drosophila* embryos: analysis of *armadillo, fused, giant*, and *unpaired* mutations in mosaic embryos. *Wilhelm Roux Arch devl Biol.* **195**, 49–62.

JERKA-DZIADOSZ, M. & FRANKEL, J. (1979). A mutant of *Tetrahymena thermophila* with a partial mirror-image duplication of cell surface pattern. I. Analysis of the phenotype. *J. Embryol. exp. Morph.* **49**, 167–202.

KALTHOFF, K. (1979). Analysis of morphogenetic determinants in the insect embryo (*Smittia* spec., Chironomidae, Diptera). In *Determinants of Spatial Organization* (ed. S. Subtelny & I. R. Konigsberg), pp. 97–126. New York: Academic Press.

LANSING, T. J., FRANKEL, J. & JENKINS, L. M. (1985). Oral ultrastructure and oral development in the misaligned undulating membrane mutant of *Tetrahymena thermophila*. *J. Protozool.* **32**, 126–139.

MOHLER, J. & WIESCHAUS, E. (1986). Dominant maternal-effect mutations of *Drosophila melanogaster* causing the production of double-abdomen embryos. *Genetics* **112**, 803–822.

NANNEY, D. L. (1966a). Corticotypes of *Tetrahymena pyriformis*. *Am. Nat.* **100**, 303–318.

NANNEY, D. L. (1966b). Corticotype transmission in *Tetrahymena*. *Genetics* **54**, 955–968.

NANNEY, D. L. (1967). Cortical slippage in *Tetrahymena*. *J. exp. Zool.* **166**, 163–170.

NANNEY, D. L., CHOW, M. & WOZENCRAFT, B. (1975). Considerations of symmetry in the cortical integration of doublets. *J. exp. Zool.* **193**, 1–14.

NELSEN, E. M. & DEBAULT, L. E. (1978). Transformation in *Tetrahymena thermophila*: description of an inducible phenotype. *J. Protozool.* **25**, 113–119.

NELSEN, E. M. & FRANKEL, J. (1986). Intracellular pattern reversal in *Tetrahymena thermophila*. I. Evidence for reverse intercalation in unbalanced doublets. *Devl Biol.* **114**, 53–71.

NELSEN, E. M., FRANKEL, J. & MARTEL, E. (1981). Development of the ciliature of *Tetrahymena thermophila*. I. Temporal coordination with oral development. *Devl Biol.* **88**, 27–38.

NG, S. F. (1979). The precise site of origin of the contractile vacuole pore in *Tetrahymena* and its morphogenetic implications. *Acta Protozool.* **18**, 305–312.

SANDER, K. (1960). Analyse des ooplasmatichen Reaktionssystems von *Euscelis plejibus* Fall. II. Die Differenzierungsleistungen nach Verlagern des Hinterpolmaterial. *Wilhelm Roux Arch. EntwMech. Org.* **151**, 660–707.

SOKAL, R. R. & ROHLF, F. J. (1981). *Biometry*, 2nd edn. San Francisco: Freeman.

SONNEBORN, T. M. (1963). Does preformed cell structure play an essential role in cell heredity? In *The Nature of Biological Diversity* (ed. J. M. Allen), pp. 165–221. New York: McGraw-Hill.

STERN, C. (1954). Two or three bristles. *Amer. Scient.* **42**, 213–247.

STERN, C. (1968). *Genetic Mosaics and Other Essays*. Cambridge, MA: Harvard University Press.

TOKUNAGA, C. (1978). Genetic mosaic studies of pattern formation in *Drosophila melanogaster*, with special reference to the prepattern hypothesis. In *Genetic Mosaics and Cell Differentiation* (ed. W. Gehring), pp. 157–204. New York: Springer-Verlag.

WINFREE, A. T. (1980). *The Geometry of Biological Time*. New York: Springer-Verlag.

WOLPERT, L. (1971). Positional information and pattern formation. *Curr. Top. devl Biol.* **6**, 183–224.